

# Biodegradable laminated poly(butylene adipate-co-terephthalate) (PBAT)/grasshopper protein-based multilayer films coated with chitosan/beeswax/baicalein for active packaging

Zisen Zhang<sup>a,\*</sup>, Changqing Fang<sup>b,\*</sup>, Xiaojuan Zhang<sup>b</sup>, Wei Zhang<sup>b</sup>, Dong Wang<sup>b</sup>

<sup>a</sup> School of Mechanical Engineering, Baoji University of Arts and Sciences, Baoji, Shaanxi 721016, PR China

<sup>b</sup> Faculty of Printing, Packing Engineering and Digital Media Technology, Xi'an University of Technology, Xi'an, Shaanxi 710048, PR China

## ARTICLE INFO

### Keywords:

Edible insect protein  
Antibacterial film  
Coating  
Biopolymers  
Food packaging

## ABSTRACT

A biodegradable multilayer film was fabricated through hot-pressing, utilizing poly(butylene adipate-co-terephthalate) (PBAT) as the barrier layer and grasshopper protein-based ternary blends as the core material, with a chitosan/beeswax/baicalein coating constructed on the surface of laminated film to achieve good antibacterial property. The test results revealed that the laminated film exhibited exceptional mechanical performance, including a tensile strength of 11.18 MPa and an elongation at break of 458.6 % with barrier properties significantly improved. Finally, the inner surface of multilayer film showed good hydrophobicity (the maximum water contact angle was 111.7°) and antibacterial activity on *S. aureus* and *Escherichia coli*. after introduction of chitosan/beeswax/baicalein coating. Moreover, the multilayer film exhibited good soil degradation rate within four weeks. This study confirmed the potential application value of grasshopper protein-based film for active packaging and proved that multilayer film technique was an excellent means to enhance physicochemical properties of natural biopolymers.

## 1. Introduction

According to BCG's report (Morach et al., 2021), the emerging alternative proteins could account for at least 11 % of total protein consumption by 2035, growing more than seven times the current market capacity to about \$290 billion, which would address the nutrient supply pressure and reduce global greenhouse gas emissions. Edible insects, recognized for their nutritional richness, low farming barriers, high resource conversion efficiency, and environmental sustainability forming circular economy systems, emerged as a key focus in alternative protein research since they were first proposed as a new earth-saved food in the FAO report in 2013 (Ordoñez-Araque et al., 2022). Following the regulatory approval in food market by EU and Singapore government, continuing concerns about the safety of edible insects have been resolved, with the current global market reached over \$3 billion and projected for substantial growth to \$17.6 billion by 2032 (Statista 2022). Biopolymers, derived from biological organisms, have emerged as principal raw materials for sustainable packaging alternatives to traditional petroleum-based packaging, owing to their excellent biocompatibility, degradability, and renewability. The plastic restriction

orders promoted by over 60 countries and growing environmental awareness of consumers have fueled the market demand for biopolymer packaging, with global production volume projected to 12.58 million tonnes in 2025 (Mordor Intelligence Research and Advisory 2024). In addition to showing great promise in food and feed industry, edible insects are excellent sources of raw materials for natural biopolymers. Previously, we proved the excellent film-forming properties of edible grasshopper protein (GP) and successfully prepared the antibacterial edible film based on GP/soy protein isolates (SPI)/Pullulan, confirming it as good alternative to traditional animal-derived protein gelatin in biopolymers for edible film. (Zhang et al., 2022; Zhang et al., 2023).

Multilayer technique often used in commercial packaging by laminating a variety of films with different properties into a single layered structure (Gartner et al., 2015). Through this combination, multilayer packaging with improved barrier properties, mechanical strength and sealing capacity over monolayer packaging can be prepared (Alias et al., 2022). However, the wide differences in chemical properties between each layer of materials make it impossible for commercial multilayer packaging to be recycled using traditional methods, which is not only a heavy burden on the environment but also a huge economic loss. Protein

\* Corresponding authors.

E-mail addresses: [jasonzzs24@163.com](mailto:jasonzzs24@163.com) (Z. Zhang), [fcqxaut@163.com](mailto:fcqxaut@163.com) (C. Fang).

and polysaccharide biopolymer are limited in many applications because of their poor mechanical properties and good hygroscopicity, while synthetic polymers usually have good barrier properties and stability. Combining both of them via multilayer technique can overcome their common defects and solve the recycling problem (Aderibigbe, 2022). Wu et al. (2021) developed the trilayer film with starch as the inner layer and PE as the outer layer, and the trilayer film improved significantly in tensile strength, water contact angle and water vapor permeability.

Compared with commonly used synthetic biodegradable biopolymers such as polylactic acid (PLA), polycaprolactone (PCL), etc., poly(butylene adipate-co-terephthalate) (PBAT) has lower price, high processability and better mechanical properties, making it a good choice for preparing laminated packaging. Compared with the traditional incorporation of antibacterial agents into the substrate, surface coating can effectively reduce the amount of antibacterial agents and maintain the physical properties of packaging materials (Fu et al., 2021). Beeswax, a natural wax secreted by honeybees and harvested from beehive, contains large amounts of esters and free fatty acids (Cornara et al., 2017). Its excellent hydrophobicity, adhesion and barrier properties make it widely used in the field of food preservation and packaging (Huang et al., 2022). Chitosan, a biopolymer ranking second in global polysaccharide abundance, is predominantly derived from chitin via deacetylation. (Huq et al., 2022). It is very suitable for antibacterial coating due to its excellent film formation, mechanical properties, antibacterial properties and non-toxicity. Baicalein, a bioactive flavone derived from the traditional Chinese herb *Scutellaria baicalensis*, exhibits effective antibacterial, antioxidant, antiviral and anti-inflammatory properties (Dong et al., 2022; Yun et al., 2022).

Although PBAT and chitosan/beeswax coatings have been extensively studied as packaging materials, their synergistic integration with insect protein-based film through multilayer technique remains under-explored. Therefore, a new biodegradable antibacterial multilayer film was developed by laminating the GP protein-based composites with barrier layer PBAT to construct sandwich structure and chitosan/beeswax/baicalein was brushed as the contacted antibacterial coating in this study. The objective is to evaluate the feasibility of producing GP protein-based composite packaging materials with fully enhanced physicochemical properties through multilayer film technique.

## 2. Materials and method

### 2.1. Materials

Frozen adult grasshoppers (*Locusta migratoria*) were purchased from a farm in Xi'an (Shannxi, China). SPI was purchased from Cool Chemical Science and Technology Co., LTD. (Beijing, China). d-xylose (98 %, Mw ~150.13) was purchased from Macklin Biochemical Co., Ltd. (Shanghai, China). Chitosan, Pullulan, Beeswax and Baicalein were purchased from Hefei Bomei Biotechnology Co., LTD. (Hefei, China). PBAT was purchased from BASF (Ludwigshafen, Germany).

### 2.2. Protein extraction

GP were extracted in the same way as described in previous study (Zhang et al., 2022).

### 2.3. Ternary blend preparation

GP/SPI/Pullulan ternary blend film was prepared according to our previous study (Zhang et al., 2023).

### 2.4. Multilayer film preparation

The pressing temperature and pressure of vulcanizing press (FR-1418, Faruiyiqi, China) was set to 140 °C and 1000 psi, respectively. The

weighted PBAT granules were placed in Teflon cloth interlayer constrained by the simple square mold and put into vulcanizing press for 3-minute hot pressing each time to obtain PBAT film as the outer layer. Then the GP/SPI/Pullulan film was wrapped by hot-pressed PBAT film and put into Teflon plate with simple square mold for 3-minute hot pressing twice at 100 °C and 1000 psi labeled as PGL. Plasma cleaning machine (TS-PL05, Tonsontec, China) was used to treat the laminated contact surface of the film at 50 °C for 30 s before lamination.

### 2.5. Coated multilayer film preparation

3 % (w/v) chitosan was dissolved in 2 % (v/v) acetic solution with 25 % (w/w) glycerol added and stirred until it was completely dissolved at 75 °C. Then 12.5 % (w/v) beeswax was added into chitosan solution and stirred for 30 min. The chitosan/beeswax complex was brushed on the surface of trilayer film and dried in the oven at 50 °C for 3 h. Above brush coating process was carried out twice to obtain coated multilayer film labeled as PGLC. 2 % Baicalein (w/v) was dispersed in chitosan/beeswax solution for 15 min to get antibacterial coated multilayer film via brush coating method labeled as PGLB. The process diagram of this experiment is shown in Fig. 1. The composition, thickness and weight data of the multilayer films represented by the abbreviations of different samples are listed in Table 1.

## 2.6. Film characterization

### 2.6.1. Scanning electron microscope (SEM)

The cryofractured samples after liquid nitrogen treatment were gold-coated through sputtering and subsequently imaged using an equipment (Jeol, JSM-6700, Japan) operated at an accelerating voltage of 3 kV.

### 2.6.2. Fourier transform infrared spectroscopy (FTIR)

Attenuated total reflectance-Fourier transform infrared (ATR-FTIR) spectrophotometer was used to analyze the chemical composition of samples at the range of 500~4000 cm<sup>-1</sup> wavenumber with a resolution of 4 cm<sup>-1</sup> and a scanning frequency of 32 times. (Vetex 70v, Bruker, Germany).

### 2.6.3. X-ray diffraction (XRD)

Multilayer films were cut into 2 × 2 cm and scanned by X-ray diffractometer (Shimadzu, XRD-7000, Japan) from 5° to 40° at 4°/min with Cu Ka source at 40 kV and 40 mA.

### 2.6.4. Thermal test

Film samples (5–10 mg) were packaged in crucibles and analyzed via an instrument (DSC 200 F3 Maia®, NETZSCH, Germany) setting temperature range of 30 °C to 100 °C at a rate of 10 °C/min to erase thermal history effects prior to testing, with the instrument configured for a full operational range of 0 °C to 200 °C.

Thermogravimetric analysis was analyzed by an instrument (TG 209 F3 Tarsus®, NETZSCH, Germany) setting temperature range at 30 °C to 550 °C.

### 2.6.5. Water vapor permeability (WVP)

Film samples were cut into 8 cm diameter and the thickness was measured by a spiral micrometer. The WVP of multilayer films were evaluated by an instrument (PERME™ W3/060, Labthink, China) setting test environment to 25 °C and 50 % RH (relative humidity).

### 2.6.6. Water contact angle (WCA)

The contact angle analysis was performed via the sessile-drop method using a measurement instrument (OCA20, Dataphysics, Germany). 2 μL of deionized water was dispensed onto five locations uniformly distributed across the flat sample surface.

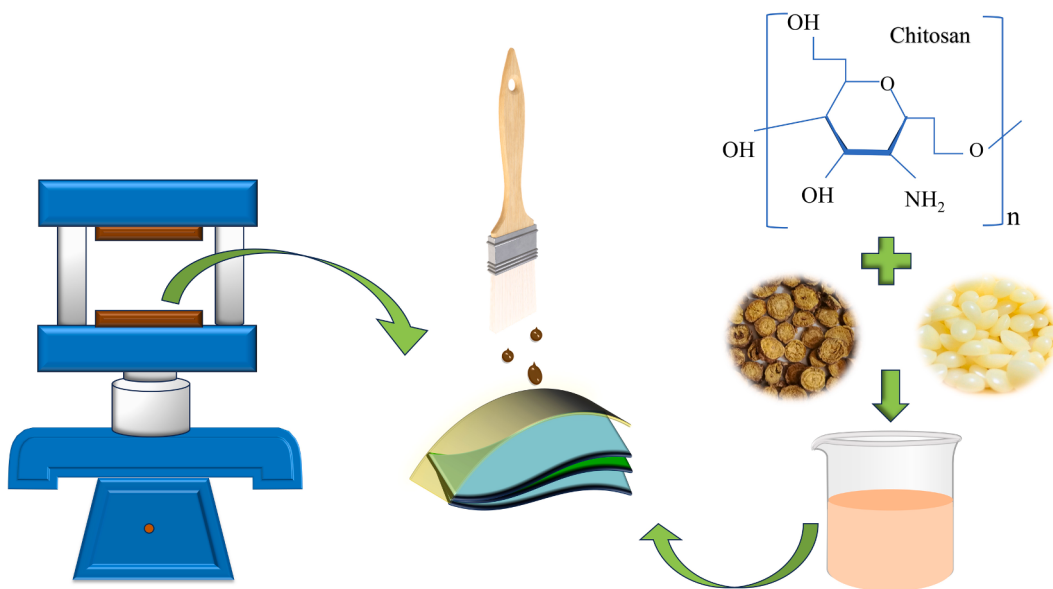


**Fig. 1.** The schematic diagram of PBAT/Grasshopper protein-based multiayers coated by chitosan-beeswax antibacterial complex.

**Table 1**  
Detailed information of multilayer films.

Sample	Inner Layer/ ratio	Outer Layer	Coating Formulation (w/v)	Thickness (mm)	Weight/cm <sup>2</sup> (mg)
Control	GP-SPI/ Pullulan (75/25)			0.46 $\pm 0.02^c$	43.2 ± 5.5 <sup>c</sup>
PGL	GP-SPI/ Pullulan (75/25)	PBAT		0.64 $\pm 0.03^b$	59.9 ± 3.9 <sup>b</sup>
PGLC	GP-SPI/ Pullulan (75/25)	PBAT	3 %Chitosan + 12.5 %Beeswax	0.91 $\pm 0.05^a$	85.9 ± 4.5 <sup>a</sup>
PGLB	GP-SPI/ Pullulan (75/25)	PBAT	3 %Chitosan+12.5 %Beeswax+2 % Baicalein	0.92 $\pm 0.05^a$	87.3 ± 6.3 <sup>a</sup>

#### 2.6.7. Mechanical properties

Film samples ( $75 \times 15$  cm) were stretched with load cell of 500 N at a speed of 20 mm/min and initial grip separation of 40 mm using Electronic Strength Tester (C610M, Labthink, China) to test their tensile strength (TS) and elongation at break (EAB).

#### 2.6.8. Antibacterial activity

The Gram-positive *S. aureus* (ATCC 6538) and Gram-negative *Escherichia coli* (ATCC 25,922) were selected and evaluated the antibacterial activity of multilayer films by inhibition zone method. The surface of the sample (12 mm diameter) was sterilized and placed in the middle of beef extract peptone medium coated with 200 mL bacterial suspension ( $10^6$  CFU/mL). All samples were put in constant temperature & humidity incubator (LHS-150HC-II, Yiheng, China) for 24 h at 37 °C and 70 % RH, then taken out to measure the diameter of antibacterial zone.

#### 2.6.9. Biodegradation test

The test sample with a diameter of 8 cm was placed in a 40-mesh screen to ensure air permeability and microorganisms exchangeability, and then buried in the soil of pH  $7.4 \pm 0.1$  at  $25^\circ\text{C} \pm 1^\circ\text{C}$  and 70 %-80 % RH in natural environment. This biodegradation test has several limitations: 1. The natural environment here refers specifically to the soil conditions within the forest area on campus, which cannot fully

simulate the complex environmental factors encountered by packaging materials in the real natural environment; 2. The sample size used in this test was relatively small, unlike the large-scale accumulation of packaging plastic waste in real garbage disposal; 3. Although a significant biodegradation trend was observed, a four-week test was still too short to fully reflect the influence of various weather conditions on packaging materials during long-term natural burial.

#### 2.7. Statistical analysis

All tests were set to be conducted at least three times, and the results obtained from the experiments are processed by SPSS Statistics 21 (IBM, New York, USA) for one-way analysis of variance (ANOVA) using Duncan multiple range test. Significant differences were determined at  $P < 0.05$ .

### 3. Results and discussion

#### 3.1. SEM

The SEM cross-section and surface scanning images of multilayer films are shown in Fig. 2(A) shows the cross-section morphology of the ternary blend material at high magnification, presenting a typical island structure, with pullulan dispersed on the substrate of the protein blend. In Fig. 2(B-D) at low magnification, the sandwich structure coated with chitosan/beeswax can be clearly seen with a rough inner layer surface stacked with spherical and spheroid dispersed phases. The binding between PGLB coating and PBAT barrier layer was tighter than PGLC and the gap was almost invisible, which is related to the presence of hydroxyl in baicalein. Hydroxyl group is an important group that affects the surface activity of coating. It played an important role in the adsorption of organic molecules and was the main reaction site for forming hydrogen bonds (Takeda et al., 1999). Kim et al. (2017) introduced a large number of hydroxyl groups into polyamide-imide coatings, and the surface adhesion of the coatings improved significantly. Matsumoto et al. (2017) found that when additives were added to pure ice to introduce hydroxyl groups, hydrogen bonds were more easily formed between the hydroxyl groups brought by the additives and the hydroxyl groups on the glass surface, and the number of hydrogen bonds increased with the increase of the number of hydroxyl groups, which would increase the shear stress between the ice and the glass surface. The surface of outer layer PBAT was smooth and uniform due to

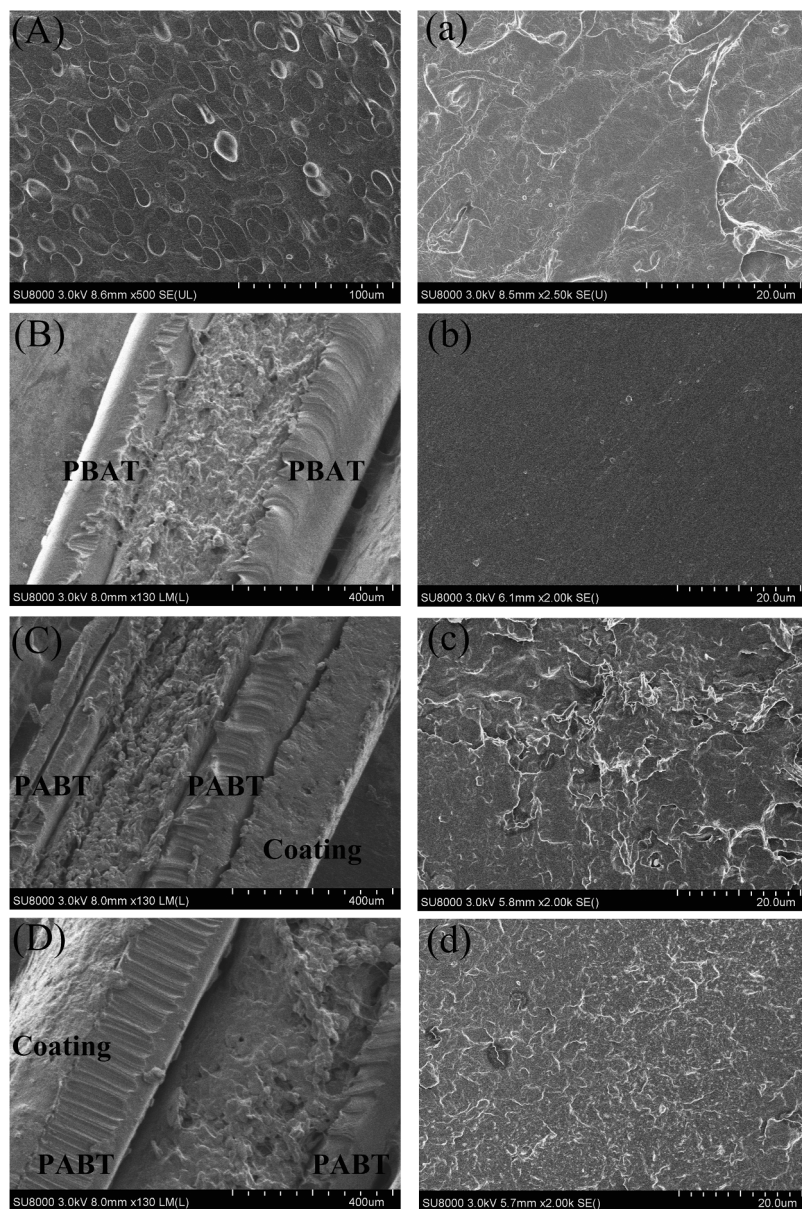


**Fig. 2.** Cross-section SEM images (A) Control (B) PGL (C) PGLC (PGLB) and surface SEM images (a)Control (b) PGL (c) PGLC (d) PGLB for PBAT/Grasshopper protein-based multilayers coated by chitosan-beeswax antibacterial complex.

repeated hot pressing in Fig. 2(b). The surface roughness of PGLB was smaller than that of PGLC, and the large lamellar protrusions were significantly reduced from Fig. 2(c-d), which may be related to the plasticizing effect of phenols.

### 3.2. FTIR

The infrared absorption spectra of multilayer films are shown in Fig. 3 (a-b). The characteristic peaks of PBAT were mainly found in PGL samples, where peak at  $726\text{ cm}^{-1}$  related to more than four adjacent methylene groups ( $-\text{CH}_2-$ ) on the main PBAT chain and small peaks between  $800\text{--}950\text{ cm}^{-1}$  were the bending peaks of benzenes (Al-Itty et al., 2012). The peak at  $1017\text{ cm}^{-1}$  was caused by the in-plane vibration of adjacent H atoms on the unique benzene ring structure of PBAT. The asymmetric and symmetric vibration modes of aliphatic and aromatic ester bonds accounted for the C—O stretching vibration of the ester bond in PBAT producing multiple absorption between  $1100$  and  $1300\text{ cm}^{-1}$ , and small dense peaks between  $1340$  and  $1580\text{ cm}^{-1}$  ascribed to the C—H bending vibration (Bumbudsanpharoke et al., 2022). The peak at  $1710$

$\text{cm}^{-1}$  related to the vibration of the carbonyl group ( $C=O$ ) of ester bond in the crystalline zone (Platnieks et al., 2020). The peak at  $2960\text{ cm}^{-1}$  was caused by the stretch vibration of C—H contained within methylene and methyl groups ( $-\text{CH}_3-$ ) (Leelaphiwat et al., 2022).

Some main chemical groups of chitosan and beeswax were observed in PGLC samples. The double-headed peak at  $723\text{ cm}^{-1}$  and sharp peak at  $1460\text{ cm}^{-1}$  both corresponded to the  $-\text{CH}_2-$  vibration, and the absorption peak at  $1165\text{ cm}^{-1}$  came from the C—H bending vibration of the single ester in beeswax (Tanner et al., 2019). The at  $1736\text{ cm}^{-1}$  was caused by the asymmetric and symmetrical stretching  $\text{C}=\text{O}$  stretching, and the two long spikes at  $2848\text{ cm}^{-1}$  and  $2914\text{ cm}^{-1}$  attributed to long hydrocarbon chains ( $\text{CH}_3$  and  $\text{CH}_2$ ) with polar head containing ester groups in beeswax (Cruces et al., 2021). The wide peak at  $1060\text{ cm}^{-1}$  was derived from the C—O skeletal stretching in chitosan as a typical saccharide structural feature (Liu et al., 2017). The C—N stretching at  $1378\text{ cm}^{-1}$  and N—H bending vibrations at  $1558\text{ cm}^{-1}$  corresponded to the amide III and amide II structures in chitosan, respectively (Bilbao-Sainz et al., 2017). FTIR results revealed that no new functional groups were generated during the lamination and coating processes, indicating that

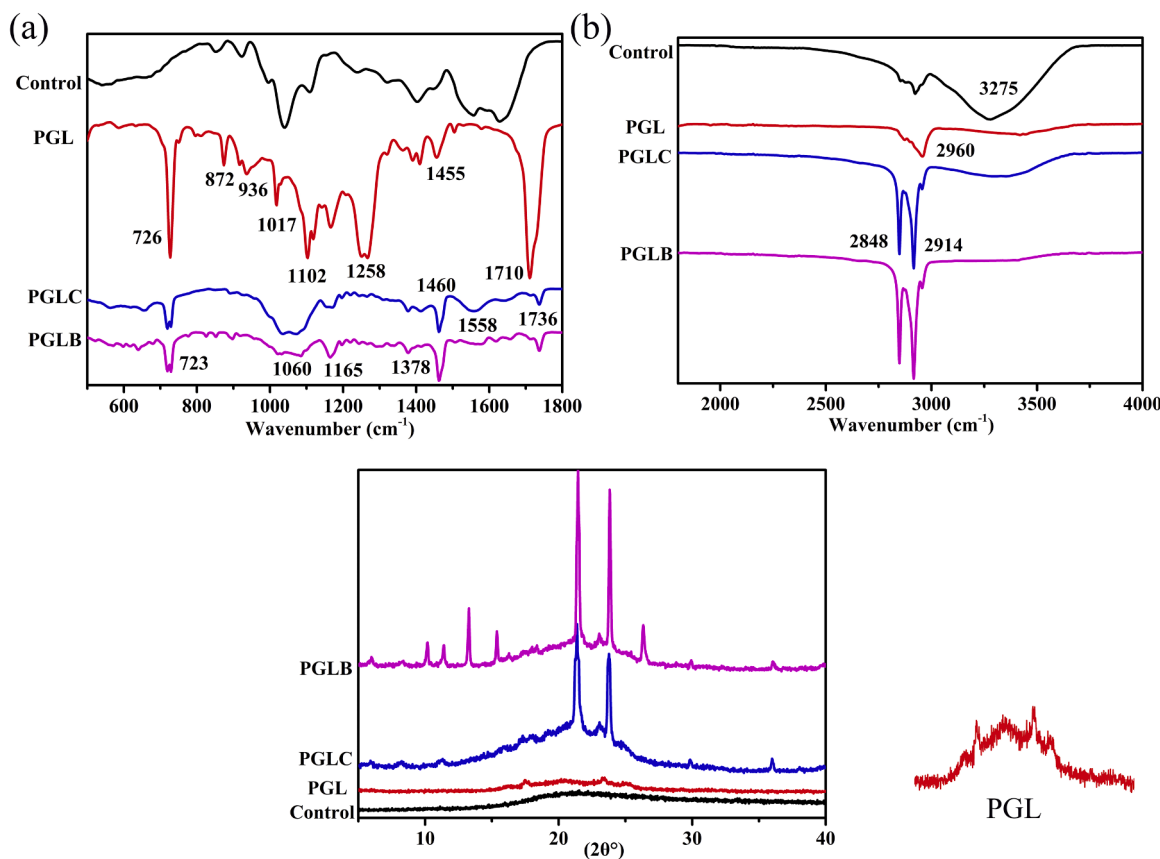


**Fig. 3.** ATR-FTIR spectra region from (a) 500–1800 cm<sup>-1</sup> (b) 500–4000 cm<sup>-1</sup> and (c) XRD patterns of PBAT/Grasshopper protein-based multilayers coated by chitosan-beeswax antibacterial complex.

interlayer bonding mainly occurred through physical interaction. And incorporation of baicalein did not undergo chemical reactions with chitosan and beeswax coating.

### 3.3. XRD

As shown in Fig. 3(c), there are five small peaks of low intensity at 16.2°, 17.4°, 20.3°, 23.4° and 24.9° in PGL samples corresponding to the (011), (010), (110), (100) and (111) crystal planes respectively, representing the  $\alpha$ -form triclinic crystalline morphology of PBAT (Iribarren et al., 2023). The crystal structure of PBAT is formed by the mixed crystallization of BT and BA units, in which the BA unit is incorporated into the BT lattice (Jiao et al., 2020). The long fingerprint peaks of beeswax crystals at 21.4° and 23.8° were the short spacing of the fatty acid chain at 4.2 Å and 3.8 Å, consisting of methyl (-CH<sub>2</sub>-) groups within the hydrocarbon chain of beeswax, confirming the existence of the orthorhombic metastable polymorph ( $\beta'$ ) structure in PGLC samples (Cruces et al., 2021; Shirvani et al., 2022). The maximum diffraction peak of chitosan was between 20° and 23° overlapping with the main diffraction peak of beeswax and other small peaks at 8.3°, 11.3° and 18°, representing its internal hydrated crystal structure of chitosan (Liu et al., 2017). Several small peaks appeared at 10.1°, 11.4°, 13.3°, 15.3° and 26.3° on PGLC, which were consistent with the typical diffraction peaks of baicalein powder (Yan et al., 2015), indicating that baicalein had stable structure after dispersing in chitosan/beeswax solution at 75 °C and did not undergo chemical reaction with coating substrates. The stable structure of baicalein ensures the good performance of the multilayer film in the subsequent antibacterial experiments. The coexistence of different crystalline phases without new diffraction peaks indicated no new chemical complex formed, which also supported conclusion of physical interaction in FTIR.

### 3.4. Thermal properties

The DSC and TG data of multilayer films are described in Fig. 4 and Table 2. In Fig. 4(a), both PGLC and PGLB samples had a very strong endothermic peak at about 63 °C, corresponding to the melting point of beeswax component in the coating layer. During the melting process, the beeswax underwent a polymorphic phase transition, first from the orthorhombic phase to the rotator phase, and then the conformation of the -CH<sub>2</sub>- chains changed from *all-trans* to *gauche-trans* (Gaillard et al., 2011). The wide heat absorption region between 110 °C and 150 °C may be the result of the combined heat absorption of PBAT melting and the glass transition of the inner ternary blend film, as well as the glass transition of chitosan component in the coating layer. Qiao et al. (2017) and Dong et al. (2004) reported the still controversial glass transition temperatures of chitosan at 105 °C and 140–150 °C, respectively.

As can be seen from Fig. 4(b), the pure PBAT film exhibited excellent thermal stability with almost no mass loss below 350 °C, and presented one-step volatilization within a narrow temperature range of 350–430 °C. While both control group and multilayer samples finished thermal decomposition in three stages. In the first stage below 180 °C, the main weight loss was caused by the volatilization of small molecules (water and plasticizers); the maximum weight loss happened in the second stage, generally occurring between 180–400 °C, and the main chain of biopolymers began to pyrolyze; the final stage was associated with the breaking of some strong bonds within polymer chains (Trujillo-de Santiago et al., 2014; Roy et al., 2020). Compared with the control group, the T<sub>10</sub> and T<sub>50</sub> of PGL samples were increased to 206.6 °C and 393.6 °C, respectively, indicating that the thermal stability of multilayer packaging was improved after lamination. The T<sub>10</sub> and T<sub>50</sub> of PGLC decreased slightly compared with PGL, indicating that the introduction of coating impaired the thermal stability of multilayer packaging. This

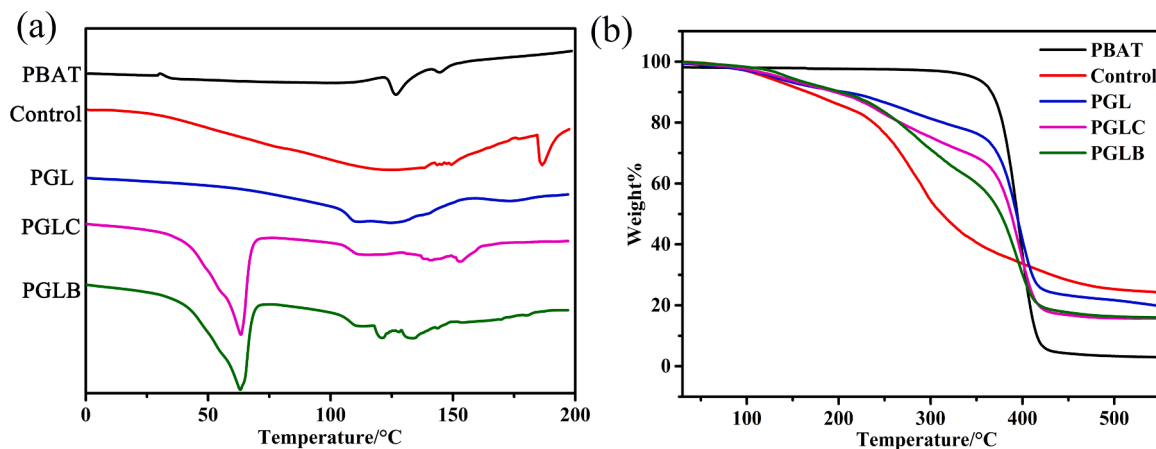


**Fig. 4.** (a) DSC and (b) TG curves of PBAT/Grasshopper protein-based multiayers coated by chitosan-beeswax antibacterial complex.

**Table 2**

Thermal stability data of PBAT/Grasshopper protein-based multiayers coated by chitosan-beeswax antibacterial complex.

Sample	T <sub>10</sub> (°C)	T <sub>50</sub> (°C)	Mass loss (%)
Control	166.4	312.3	24.3
PBAT	366.2	394.3	2.9
PGL	206.6	393.6	19.9
PGLC	196.1	387.9	15.7
PGLB	202.3	376.2	16.0

T<sub>10</sub> and T<sub>50</sub> represent the temperature corresponding to the pyrolysis of 10 % and 50 % of materials, respectively.

may be related to the volatilization of beeswax in the second stage, during which beeswax rapidly lost almost all its mass in a one-step degradation starting from 200 °C (Huang et al., 2022). After baicalein were added into the coating, the thermal stability of multilayer film in the second stage was further deteriorated, with T<sub>50</sub> dropping to 376.2 °C. As a phenolic compound, the steric hindrance effect generated by the addition of baicalein can hinder the interaction between chitosan chains, and it migrated to heat-sensitive free radicals, causing the polymer network to undergo thermal degradation at lower temperatures (Riaz et al., 2018; Nguyen et al., 2020).

### 3.5. WVP

Protein-based materials generally have poor barrier properties to polar substances such as water vapor, which was associated with the high content of hydrophilic amino acid residues and good water solubility of most protein materials (Wittaya, 2012). As the data shown in Fig. 5(a), when PBAT was laminated into a three-layer composite film

with the control group as a water-blocking layer, the WVP of new multilayer film was changed by orders of magnitude, decreasing from  $1.94 \times 10^{-11}$  to  $6.68 \times 10^{-13}$  (g/cm·s·Pa). The multilayer structure was equivalent to the establishment of continuous barrier walls, significantly extending the staying time of permeable molecules in the multilayer films, thus played a certain delayed effect (Huang et al., 2023). After the multilayer film surface was brushed with chitosan/beeswax coating, the WVP was further declined to  $4.39 \times 10^{-13}$  (g/cm·s·Pa). The hydrophobic components in beeswax played a key role here, ensuring less water adsorption in the coating, and lipid ingredient prolonged the water transport path compared with hydrophilic substances (Sun et al., 2021). In addition to the good film-forming effect, chitosan had a positive effect on WVP of coating. Zhang et al. (2014) put special emphasis on the synergistic interaction between chitosan and beeswax, and observed that the same WVP effect can be achieved with the application of chitosan/beeswax coating only about half of the weight of the theoretical pure beeswax coating.

### 3.6. WCA

The WCA data of multilayer films are summarized in Fig. 5(b). By constructing a three-layer sandwich like structure and using PBAT as the outer barrier layer, the WCA of multilayer packaging can reach 68.4°, presenting a relatively hydrophobic state. After the introduction of chitosan/beeswax as a hydrophobic coating, the WCA of PGLC samples were further increased to 111.7°. The WCA of pure chitosan film is usually between 60° and 100°, and the hydrophobic groups in beeswax such as long-chain fatty alcohols and alkanes were exposed to air to interfere with the water molecule arrangement, ensuring the hydrophobicity of entire coating together (Sun et al., 2021). The WCA of PGLB decreased to 93.1°, confirming the negative effect of baicalein on

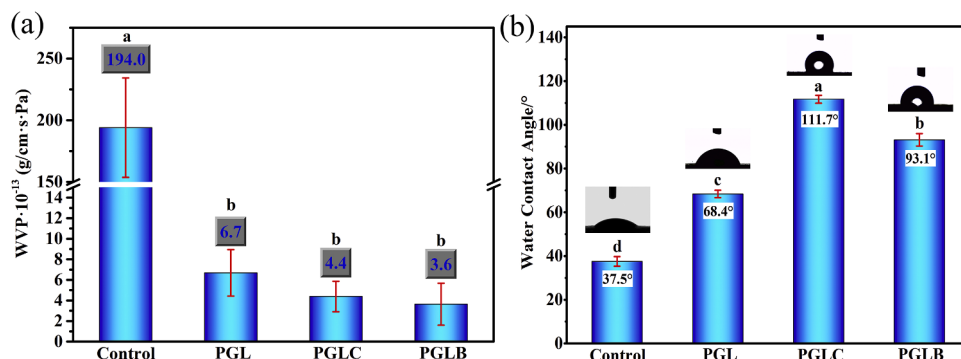


**Fig. 5.** (a) WVP (b) WCA of PBAT/Grasshopper protein-based multiayers coated by chitosan-beeswax antibacterial complex.

hydrophobicity of coating, which was related to the presence of hydrophilic hydroxyl groups inside baicalein.

### 3.7. Mechanical properties

The TS and EAB data of the multilayer film are depicted in Fig. 6. The fracture of multilayer films can be clearly observed during the stretching process through the following steps: The inner and outer layer materials were stretched uniformly and simultaneously, transferring part of the load borne by the inner layer matrix to the outer PBAT layer through the interface. When stretched to a certain extent, the weak inner layer was pulled apart in a continuous N-shaped zigzag pattern. Finally, when the inner layer was pulled apart completely, the inner and outer layers would separate. Compared with control group, the TS and EAB of PGL increased to 11.18 MPa and 458.6 %, respectively. Rakotonirainy et al. (2001) mentioned that the lamination technique enhanced the tensile property of materials by increasing the film density, optimizing the melt-flow behaviour of the film, and mitigating film structural imperfections such as pinholes and cracks. The adhesion of the chitosan/beeswax coating was not good enough so that it would soon fall off when the coated multilayer film deformed greatly with no function of bearing the load. Therefore, when PGCL and PGLB were stretched, the loading-bearing matrix was still PGL part, and the increase of thickness led to the decrease of TS when the maximum tensile force remained unchanged. According to result of Song et al. (2022), the mechanical properties of the PET/Whey Protein Isolates/LLDPE multilayer films they developed were superior to PET/AlO<sub>x</sub>/LLDPE, where the coating had no effect on the mechanical properties of multilayer film and thicker PET resulted in better mechanical properties. Therefore, combined with the tensile test results of this experiment, the relative thickness ratio between each functional layer was crucial in the preparation of multilayer films with good mechanical properties. If coating technology was used, it is necessary to control the coating thickness.

### 3.8. Antibacterial properties

Although a large number of previous studies confirmed that chitosan was a biopolymer with good antibacterial activity, it can be seen from Fig. 7 that PGCL samples showed no antibacterial zone. This may be influenced by varieties of factors: One is that beeswax in chitosan/beeswax coating had a lower density than chitosan, so that it distributed more on the top of the coating when it solidified. Another is depended on the type of chitosan, which differed in extraction sources, viscosity, molecular weight and degree of deacetylation. Tanpichai et al. (2020) also obtained similar experimental results to ours. When they used 1 % concentration of high molecular weight and low molecular weight chitosan film forming liquid to conduct antibacterial experiments on *S. aureus* and *E. coli*, only low molecular weight chitosan film forming

liquid was observed to present antibacterial activity. While the low molecular weight chitosan film forming liquid was coated on the paper, the antibacterial activity was completely lost. They speculated that the solidification of chitosan solution may lose a large number of active cationic amino groups which were thought to play a key role in the antibacterial mechanism of chitosan. Ojagh et al. (2010) also confirmed that pure chitosan films did not show antibacterial activity against five microorganisms including *L. monocytogenes* and *E. coli*, which may be due to the fact that no migrating antibacterial agent was added into the chitosan films, failing to spread out with the agar, and the antibacterial ability brought by its own structure can only be displayed in direct contact with microorganisms. After adding baicalein, the multilayer film exhibited significant antibacterial efficacy, with an inhibition zone diameter of 23.5 mm observed against *S. aureus*, which was higher than that of *E. coli* due to the extra lipopolysaccharide protective layer. The antibacterial mechanism of baicalein was complicated. Chen et al. (2016) found that baicalein significantly inhibited the biofilm growth of *S. aureus* and the system controlling the release of virulence factors. Chen et al. (2013) studied the antibacterial mechanism of *S. aureus* and concluded that baicalein had limited damage to cell membrane, which was not enough to cause the leakage of large molecules such as DNA and RNA, while it achieved the antibacterial purpose by inhibiting the activity of key enzymes on DNA and destroying the normal replication and transcription process of cells. From the perspective of baicalein's own structure and group composition, C<sub>4</sub>=O, C<sub>5</sub>-OH and C<sub>7</sub>-OH are the three most active groups that play the most antibacterial role. After interacting with bacteria, hydroxyl can bind with amino or carboxyl groups in its protein molecules, and its hydrophobic benzene ring may also bind with proteins (Ouyang et al., 2017).

### 3.9. Biodegradation

Generally, the degradation of polymers in soil can be divided into five steps: biodegradation, depolymerization, identification, assimilation, and mineralization (Shaikh et al., 2021). As can be seen from Fig. 8, PBAT was very stable in 4-week time under natural environment, and the existence of ester bonds on its benzene ring makes it difficult to be hydrolyzed. Huang et al. (2022) reported that PBAT was difficult to degrade within 14 weeks in soil and its weight loss rate was close to only 2.1 %. Zhai et al. (2023) got the soil degradation experiment results that PBAT had a weight loss rate of only about 10 % within 180 days. In contrast, the protein-polysaccharide film of the control group was almost degraded by >90 % in 3 days in the moist soil and a large number of white molds could be seen on the surface. After lamination, PGL samples showed a good degradation rate in the soil degradation test, and nearly half of its weight were lost within four weeks. The plentiful nitrogen excellent and carbon sources in protein-polysaccharide of

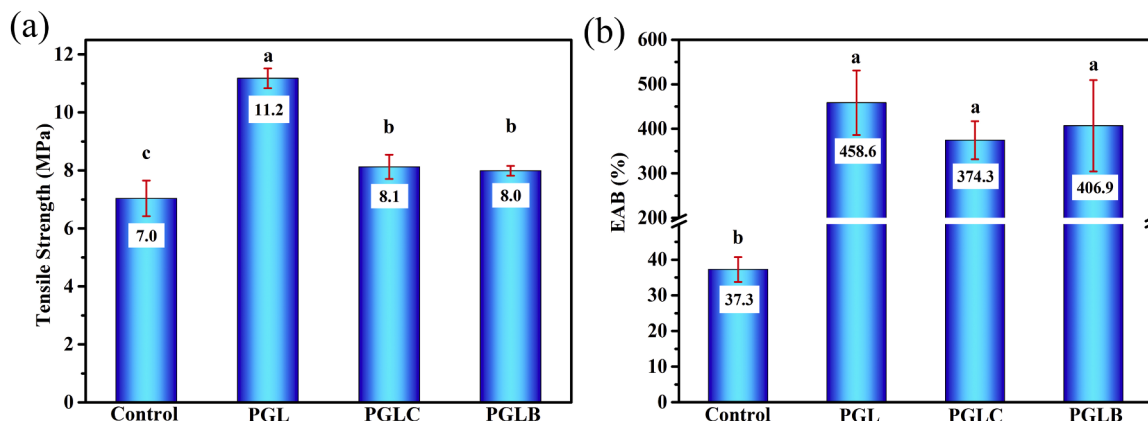
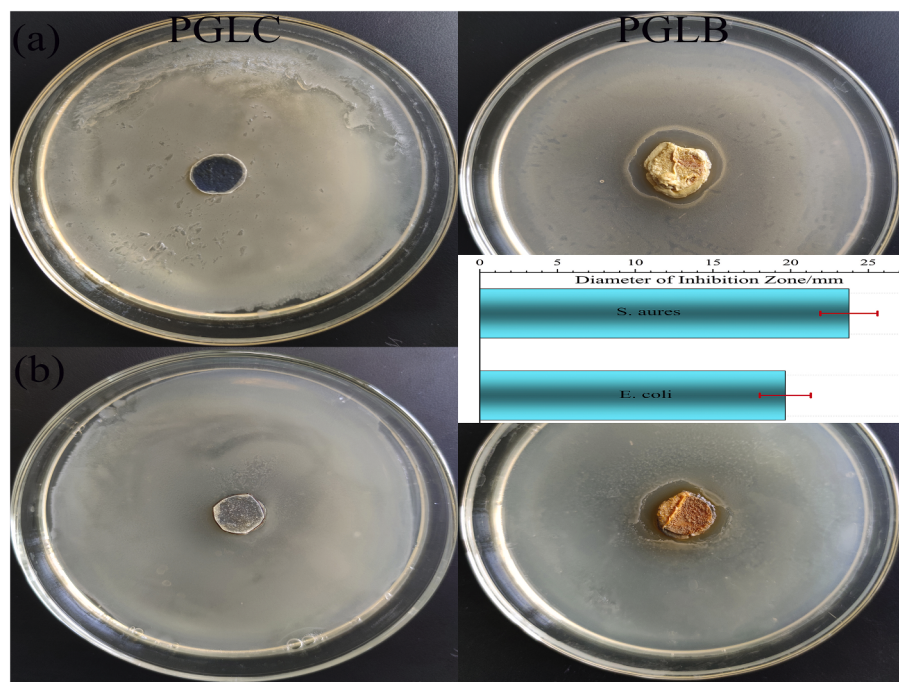
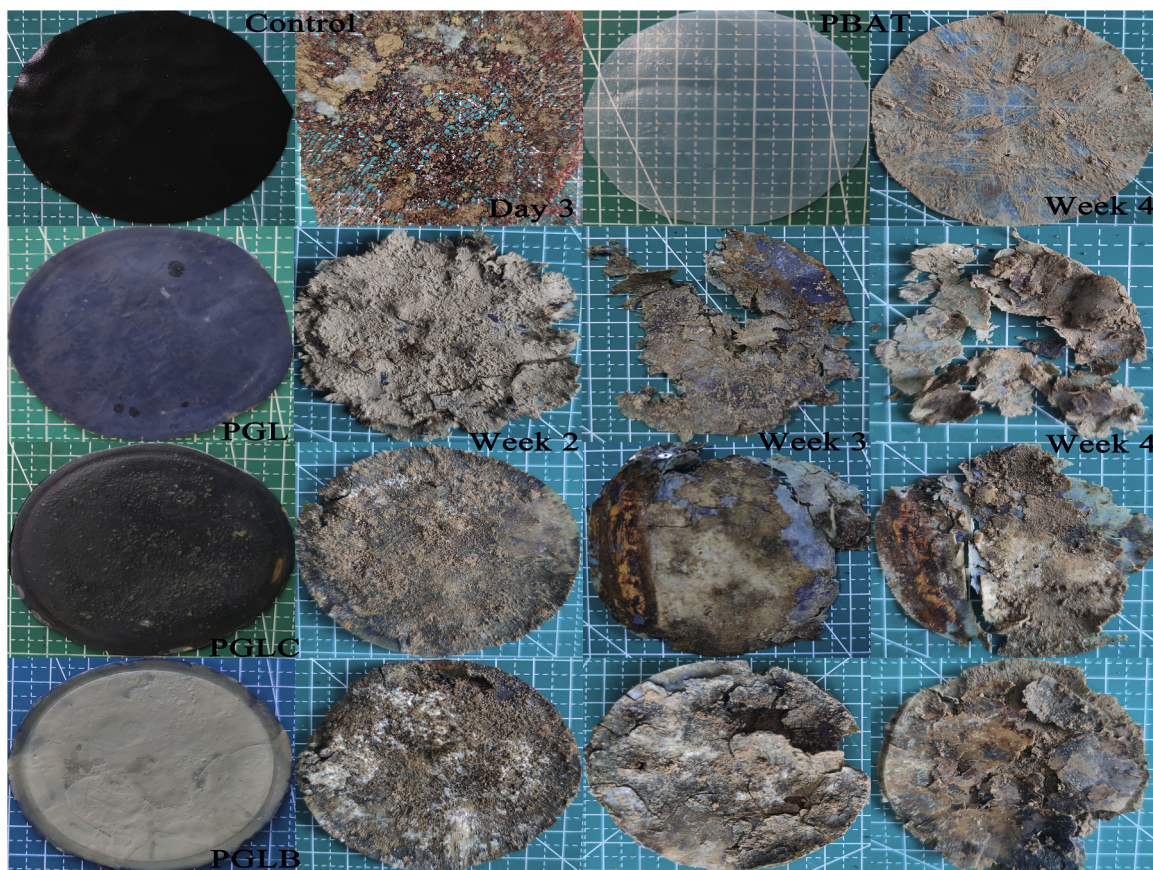


Fig. 6. (a) TS (b) EAB of PBAT/Grasshopper protein-based multilayers coated by chitosan-beeswax antibacterial complex.



**Fig. 7.** The inhibition zones of PBAT/Grasshopper protein-based multiayers coated by chitosan-beeswax antibacterial complex against (a) *S. aureus* and (b) *E. coli*.



**Fig. 8.** Soil biodegradation test of PBAT/Grasshopper protein-based multiayers coated by chitosan-beeswax antibacterial complex.

interlayer films became an excellent food source for microorganisms in the soil, creating a large number of active sites, and providing more opportunities for the hard-to-degrade PBAT outlayer film to come into contact with microorganisms. As can be seen from Fig. 8, the

degradation of multilayer films started from the edge of the film, because the interlayer films at the edge were exposed to microorganisms in direct contact with the soil, and the enzymes secreted by the micro-organisms accelerated the whole film degradation contacting with PBAT

outlayer film. However, the degradation rate of PGLC decreased due to the hydrophobicity of chitosan/beeswax coating. The process of microorganisms secreting enzyme on degradation of polymer was more hydrophilic, and the polymer after water absorption would be more unstable and conducive to degradation (Doh et al., 2020). PGLB degraded more slowly than PGLC, which may be related to the antimicrobial properties of baicalein. The surface of PGLB still have an inhibitory effect on some microorganisms in the early stage of degradation, thus the number and types of microorganisms on the film surface are relatively less. Boeira et al. (2022) also observed that the addition of corn stigma extract to gelatin-based edible film slowed the degradation rate of the material because the antioxidant properties of phenolic substances affected the activity of microorganisms in the environment. For packaging materials with slow degradation rate, it is an option to improve their degradability in natural environment by combining with protein-based biopolymers through multilayer technique.

#### 4. Conclusion

A novel antibacterial and biodegradable multilayer packaging film was developed by combining grasshopper protein-based composites with PBAT through hot pressing and coating techniques, further confirming the excellent processing plasticity of grasshopper protein as biopolymers. This approach significantly enhanced mechanical properties, with TS and EAB reaching 11.18 MPa and 458.6 %, respectively, while also improving barrier properties, surface hydrophobicity and thermal stability. With chitosan/beeswax complex coated onto the surface of laminated film, the WCA increased to 111.7° and WVP reduced to  $4.39 \times 10^{-13}$  (g/cm·s·Pa). Furthermore, the multilayer film showed excellent growth inhibition ability against *S. aureus* and *E. coli* by adding 2 % baicalein to the coating. In a four-week soil biodegradation test, the trilayer film exhibited a relatively fast degradation rate losing nearly half of the weight, while the construction of coating layer slowed down the degradation rate of multilayer film. It is hoped that future studies will include toxicity and allergenicity tests for grasshopper protein-based materials to ensure their safety as food packaging.

#### CRediT authorship contribution statement

**Zisen Zhang:** Writing – original draft, Methodology, Investigation, Data curation, Conceptualization. **Changqing Fang:** Resources, Project administration, Funding acquisition. **Xiaojuan Zhang:** Writing – review & editing, Supervision. **Wei Zhang:** Resources, Methodology. **Dong Wang:** Writing – review & editing, Validation, Supervision.

#### Declaration of competing interest

We declare that we have no financial and personal relationships with other people or organizations that can inappropriately influence our work, there is no professional or other personal interest of any nature or kind in any product, service and/or company that could be construed as influencing the position presented in, or the review of, the manuscript entitled.

#### Ethical statement - studies in humans and animals

This study involved no tests on humans or on animals.

#### Acknowledgement

The authors acknowledge the financial support provided by the National Natural Science Foundation of China (Grant No. 51802259).

#### Data availability

Data will be made available on request.

#### References

- Aderibigbe, B.A., 2022. Hybrid-based wound dressings: combination of synthetic and biopolymers. *Polymers* 14 (18), 3806. <https://doi.org/10.3390/polym14183806>.
- Alias, A.R., Khairul Wan, M., Sarbon, N.M., 2022. Emerging materials and technologies of multi-layer film for food packaging application: a review. *Food Control* 136, 108875. <https://doi.org/10.1016/j.foodcont.2022.108875>.
- Al-Ittry, R., Lamnawar, K., Maazouz, A., 2012. Improvement of thermal stability, rheological and mechanical properties of PLA, PBAT and their blends by reactive extrusion with functionalized epoxy. *Polym. Degrad. Stab.* 97 (10), 1898–1914. <https://doi.org/10.1016/j.polymdegradstab.2012.06.028>.
- Bilbao-Sainz, C., Chiou, B.S., Williams, T., Wood, D., Du, W.X., Sedej, I., Ban, Z., Rodov, C., Poverenov, E., Vinokur, Y., McHugh, T., 2017. Vitamin D-fortified chitosan films from mushroom waste. *Carbohydr Polym*. 167, 97–104. <https://doi.org/10.1016/j.carbpol.2017.03.010>.
- Boeira, C.P., Flores, D.C.B., Alves, J.D., de Moura, M.R., Melo, P.T.S., Rolim, C.M.B., Nogueira-Librelootto, D.R., da Rosa, C.S., 2022. Effect of corn stigma extract on physical and antioxidant properties of biodegradable and edible gelatin and corn starch film. *Int. J. Biol. Macromol.* 208, 698–706. <https://doi.org/10.1016/j.ijbiomac.2022.03.164>.
- Bumbudsanpharoke, N., Wongphan, P., Promhuad, K., Leelaphifat, P., Harnkarnsujarit, N., 2022. Morphology and permeability of bio-based poly(butylene adipate-co-terephthalate) (PBAT), poly(butylene succinate) (PBS) and linear low-density polyethylene (LLDPE) blend films control shelf-life of packaged bread. *Food Control* 132, 108541. <https://doi.org/10.1016/j.foodcont.2021.108541>.
- Chen, Y., Liu, T., Wang, K., Hou, C., Cai, S., Huang, Y., Du, Z., Huang, H., Kong, J., Chen, Y., 2016. Baicalein inhibits *Staphylococcus aureus* biofilm formation and the quorum sensing system *In vitro*. *Plos One*. 11 (4), e0153468. <https://doi.org/10.1371/journal.pone.0153468>.
- Chen, Y., Tong, Z., Xie, K., Yun, B., Xie, M., 2013. Antibacterial mechanism of Baicalein on methicillin-resistant *staphylococcus aureus*. *Acta Veterinaria et Zootechnica Sinica* 44 (12), 2000–2006.
- Cornara, L., Biagi, M., Xiao, J., Burlando, B., 2017. Therapeutic properties of bioactive compounds from different Honeybee products. *Front Pharmacol.* 8, 412. <https://doi.org/10.3389/fphar.2017.00412>.
- Cruces, F., García, M.G., Ochoa, N.A., 2021. Reduction of water vapor permeability in food multilayer biopackaging by epitaxial crystallization of beeswax. *Food Bioproc. Tech.* 14. <https://doi.org/10.1007/s11947-021-02628-9>, 1244–1255.
- Doh, H., Dunno, K.D., Whiteside, W.S., 2020. Cellulose nanocrystal effects on the biodegradability with alginate and crude seaweed extract nanocomposite films. *Food Biosci.* 38, 100795. <https://doi.org/10.1016/j.fbio.2020.100795>.
- Dong, Y., Sui, L., Yang, F., Ren, X., Xing, Y., Xiu, Z., 2022. Reducing the intestinal side effects of acarbose by baicalein through the regulation of gut microbiota: an *In vitro* study. *Food Chem.* 394, 133561. <https://doi.org/10.1016/j.foodchem.2022.133561>.
- Dong, Y., Ruan, Y., Wang, H., Zhao, Y., Bi, D., 2004. Studies on glass transition temperature of chitosan with four techniques. *J. Appl. Polymer Sci.* 93, 1553–1558. <https://doi.org/10.1002/app.20630>.
- Fu, Y., Dudley, E.G., 2021. Antimicrobial-coated films as food packaging: a review. *Comprehensive Rev. Food Sci. Food Safety*. 20 (4), 3404–3437. <https://doi.org/10.1111/1541-4337.12769>.
- Gaillard, Y., Mija, A., Burr, A., Darque-Ceretti, E., Felder, E., Sbirrazzuoli, N., 2011. Green material composites from renewable resources: polymorphic transitions and phase diagram of beeswax/rosin resin. *Thermochim Acta*. 521 (1–2), 90–97. <https://doi.org/10.1016/j.tca.2011.04.010>.
- Gartner, H., Li, Y., Almenar, E., 2015. Improved wettability and adhesion of polylactic acid/chitosan coating for bio-based multilayer film development. *Appl. Surf. Sci.* 332, 488–493. <https://doi.org/10.1016/j.apsusc.2015.01.157>.
- Huang, H., Huang, C., Xu, C., Liu, R., 2022a. Development and characterization of lotus-leaf-inspired bionic antibacterial adhesion film through beeswax. *Food Packaging Shelf Life* 33, 100906. <https://doi.org/10.1016/j.fpsl.2022.100906>.
- Huang, H.D., Ren, P.G., Zhong, G.J., Olah, A., Li, Z.M., Baer, E., Zhu, L., 2023. Promising strategies and new opportunities for high barrier polymer packaging films. *Prog Polym Sci.* 144, 101722. <https://doi.org/10.1016/j.progpolymsci.2023.101722>.
- Huang, C., Liao, Y., Zou, Z., Chen, Y., Jin, M., Zhu, L., Abdalkarim, S.Y.H., Zhou, Y., Yu, H.Y., 2022b. Novel strategy to interpret the degradation behaviors and mechanisms of bio- and non-degradable plastics. *J. Clean Prod.* 355, 131757. <https://doi.org/10.1016/j.jclepro.2022.131757>.
- Huq, T., Khan, A., Brown, D., Dhayagude, N., He, Z., Ni, Y., 2022. Sources, production and commercial applications of fungal chitosan: a review. *J. Bioresources Bioprod.* 7 (2), 85–98. <https://doi.org/10.1016/j.jobab.2022.01.002>.
- Iribarren, E., Wongphan, P., Bumbudsanpharoke, N., Chonhenclob, V., Jarupan, L., Harnkarnsujarit, N., 2023. Thermoplastic agar blended PBAT films with enhanced oxygen scavenging activity. *Food Biosci.* 54, 102940. <https://doi.org/10.1016/j.fbio.2023.102940>.
- Jiao, J., Zeng, X., Huang, X., 2020. An overview on synthesis, properties and applications of poly(butylene-adipate-co-terephthalate)-PBAT. *Adv. Indust. Eng. Polymer Res.* 3, 19–26. <https://doi.org/10.1016/j.aiepr.2020.01.001>.
- Kim, K., Yoo, T., Lee, J., Kim, M., Lee, S., Kim, G., Kim, J., Han, P., Han, H., 2017. The effects of hydroxyl groups on the thermal and optical properties of poly(amide-imide)s with high adhesion for transparent films. *Prog. Organ. Coat.* 112, 37–43. <https://doi.org/10.1016/j.porgcoat.2017.06.018>.
- Leelaphifat, P., Pechprakan, C., Siriphop, P., Bumbudsanpharoke, N., Harnkarnsujarit, N., 2022. Effects of nisin and EDTA on morphology and properties of thermoplastic starch and PBAT biodegradable films for meat packaging. *Food Chem.* 369, 130956. <https://doi.org/10.1016/j.foodchem.2021.130956>.

- Liu, J., Liu, S., Wu, Q., Gu, Y., Kan, J., Jin, C., 2017. Effect of protocatechuic acid incorporation on the physical, mechanical, structural and antioxidant properties of chitosan film. *Food Hydrocoll.* 73, 90–100. <https://doi.org/10.1016/j.foodhyd.2017.06.035>.
- Matsumoto, K., Tsubaki, D., Sekine, K., Kubota, H., Minamiya, K., Yamanaka, S., 2017. Influences of number of hydroxyl groups and cooling solid surface temperature on ice adhesion force. *Int. J. Refrigerat.* 75, 322–330. <https://doi.org/10.1016/j.ijrefrig.2016.12.007>.
- Mordor Intelligence Research & Advisory, 2024. Biopolymers Packaging Market Size & Share Analysis-Growth Trends & Forecasts (2025-2030). <https://www.mordorintelligence.com/industry-reports/biopolymer-packaging-market>.
- Morach, B., Witte, B., Walker, D., von Koeller, D., Grosse-Holz, F., Rogg, J., Brigitte, M., Dehnert, N., Obloj, P., Koktenturk, S., Schulze, U., 2021. Food for thought: the protein transformation. <https://www.bcg.com/ja-jp/publications/2021/the-benefits-of-plant-based-meats>.
- Nguyen, T.T., Dao, U.T.T., Bui, Q.P.T., Bach, G.L., Thuc, C.N.C., Thuc, H.H., 2020. Enhanced antimicrobial activities and physicochemical properties of edible film based on chitosan incorporated with *Sonneratia caseolaris* (L.) Engl. Leaf extract. *Prog. Organ. Coat.* 140, 105487. <https://doi.org/10.1016/j.porgcoat.2019.105487>.
- Ojagh, S.M., Rezaei, M., Razavi, S.H., Hosseini, S.M.H., 2010. Development and evaluation of a novel biodegradable film made from chitosan and cinnamon essential oil with low affinity toward water. *Food Chem.* 122, 161–166. <https://doi.org/10.1016/j.foodchem.2010.02.033>.
- Ordoñez-Araque, R., Quishpillo-Miranda, N., Ramos-Guerrero, L., 2022. Edible insects for humans and animals: nutritional composition and an option for mitigating environmental damage. *Insects* 13, 944. <https://doi.org/10.3390/insects13100944>.
- Ouyang, H., Hou, K., Ge, S., Deng, H., Peng, X., 2017. Antimicrobial activities of flavonoids against bamboo-destroying fungi and molds. *Toxicol. Environ. Chem.* 99 (5–6), 892–899. <https://doi.org/10.1080/02772248.2017.1320049>.
- Platnički, O., Barkane, A., Ijudina, N., Gaidukova, G., Thakur, V.K., Gaidukovs, S., 2020. Sustainable tetra pak recycled cellulose/poly(Butylenesuccinate) based woody-like composites for a circular economy. *J. Clean. Prod.* 270, 122321. <https://doi.org/10.1016/j.jclepro.2020.122321>.
- Qiao, C., Ma, X., Zhang, J., Yao, J., 2017. Molecular interactions in gelatin/chitosan composite films. *Food Chem.* 235, 45–50. <https://doi.org/10.1016/j.foodchem.2017.05.045>.
- Rakotonirainy, A.M., Padua, G.W., 2001. Effects of lamination and coating with drying oils on tensile and barrier properties of zein films. *J. Agric. Food Chem.* 49 (6), 2860–2863. <https://doi.org/10.1021/jf000845u>.
- Riaz, A., Lei, S., Akhtar, H.M.S., Wan, P., Chen, D., Jabbar, S., Abid, M., Hashim, M.M., Zeng, X., 2018. Preparation and characterization of chitosan-based antimicrobial active food packaging film incorporated with apple peel polyphenols. *Int. J. Biol. Macromol.* 114, 547–555. <https://doi.org/10.1016/j.ijbiomac.2018.03.126>.
- Roy, S., Hai, V.H., Kim, C.H., Zhai, L., Kim, J., 2020. Preparation and characterization of synthetic melanin-like nanoparticles reinforced chitosan nanocomposite films. *Carbohydr Polym.* 231, 115729. <https://doi.org/10.1016/j.carbpol.2019.115729>.
- Shaikh, S., Yaqoob, M., Aggarwal, P., 2021. An overview of biodegradable packaging in food industry. *Curr. Res. Food Sci.* 4, 503–520. <https://doi.org/10.1016/j.crefs.2021.07.005>.
- Shirvani, A., Goli, S.A.H., Varshosaz, J., Salvia-Trujillo, L., Martín-Belloso, O., 2022. Fabrication of edible solid lipid nanoparticle from beeswax/propolis wax by spontaneous emulsification: optimization, characterization and stability. *Food Chem.* 387, 132934. <https://doi.org/10.1016/j.foodchem.2022.132934>.
- Song, H.G., Choi, I., Lee, J.S., Chang, Y., Yoon, C.S., Han, J., 2022. Whey protein isolate coating material for high oxygen barrier properties: a scale-up study from laboratory to industrial scale and its application to food packaging. *Food Packag. Shelf Life.* 31, 100765. <https://doi.org/10.1016/j.fpsl.2021.100765>.
- Statista, 2022. Edible Insects - statistics & facts (Published By M. Shahbandeh, Dec 14, 2022). <https://www.statista.com/topics/4806/edible-insects/#topicOverview>.
- Sun, R., Song, G.S., Zhang, H., Zhang, H., Chi, Y., Ma, Y., Li, H., Bai, S., Zhang, X., 2021. Effect of basil essential oil and beeswax incorporation on the physical, structural, and antibacterial properties of chitosan emulsion based coating for eggs preservation. *LWT - Food Sci. Technol.* 150, 112020. <https://doi.org/10.1016/j.lwt.2021.112020>.
- Takeda, S., Fukawa, M., Hayashi, Y., Matsumoto, K., 1999. Surface OH group governing adsorption properties of metal oxide films. *Thin Solid Films.* 339 (1–2), 220–224. [https://doi.org/10.1016/S0040-6090\(98\)01152-3](https://doi.org/10.1016/S0040-6090(98)01152-3).
- Tanner, N., Lichtenberg-Kraag, B., 2019. Identification and quantification of single and multi-adulteration of beeswax by FTIR-ATR spectroscopy. *Europe. J. Lipid Sci. Technol.* 121, 1900245. <https://doi.org/10.1002/ejlt.201900245>.
- Tanpichai, S., Witayakran, S., Woothikanokkhan, J., Srimarut, Y., Woraprayote, W., Malila, Y., 2020. Mechanical and antibacterial properties of the chitosan coated cellulose paper for packaging applications: effects of molecular weight types and concentrations of chitosan. *Int. J. Biol. Macromol.* 155, 1510–1519. <https://doi.org/10.1016/j.ijbiomac.2019.11.128>.
- Trujillo-de Santiago, G., Rojas-de Gante, C., Garcia-Lara, S., Verdolotti, L., Di Maio, E., Iannace, S., 2014. Strategies to produce thermoplastic starch-zein blends: effect on compatibilization. *J. Polym. Environ.* 22 (4), 508–524. <https://doi.org/10.1007/s10924-014-0685-4>.
- Wittaya, T., 2012. *Structure and Function of Food Engineering*. IntechOpen, London.
- Wu, S., Wang, W., Zhang, R., Zhai, X., Hou, H., 2021. Preparation and characterization of biodegradable trilayer films based on starch and polyester. *Int. J. Biol. Macromol.* 183, 1058–1066. <https://doi.org/10.1016/j.ijbiomac.2021.05.051>.
- Yan, T., Cheng, Y., Wang, Z., Huang, D., Miao, H., Zhang, Y., 2015. Preparation and characterization of baicalein powder micronized by the SEDS process. *J. Supercritic. Fluids* 104, 177–182. <https://doi.org/10.1016/j.supflu.2015.06.005>.
- Yun, C., Wang, S., Gao, Y., Zhao, Z., Miao, N., Shi, Y., Ri, I., Wang, W., Wang, H., 2022. Optimization of ultrasound-assisted enzymatic pretreatment for enhanced extraction of baicalein and wogonin from *Scutellaria baicalensis* roots. *J. Chromatograph. B.* 1188, 123077. <https://doi.org/10.1016/j.jchromb.2021.123077>.
- Zhai, X., Li, M., Zhang, R., Wang, W., Hou, H., 2023. Extrusion-blown starch/PBAT biodegradable active films incorporated with high retentions of tea polyphenols and the release kinetics into food simulants. *Int. J. Biol. Macromol.* 227, 851–862. <https://doi.org/10.1016/j.ijbiomac.2022.12.194>.
- Zhang, W., Xiao, H., Qian, L., 2014. Enhanced water vapour barrier and grease resistance of paper bilayer-coated with chitosan and beeswax. *Carbohydr. Polym.* 101, 401–406. <https://doi.org/10.1016/j.carbpol.2013.09.097>.
- Zhang, Z., Fang, C., Liu, D., Zhou, X., Wang, D., Zhang, W., 2022. Preparation and characterization of the protein edible film extracted from the migratory locust (*Locusta migratoria*). *Food Packag. Shelf Life.* 33, 100899. <https://doi.org/10.1016/j.fpsl.2022.100899>.
- Zhang, Z., Fang, C., Zhang, W., Lei, W., Wang, D., Zhou, X., 2023. Novel grasshopper protein/soy protein isolate/pullulan ternary blend with hesperidin derivative for antimicrobial edible film. *Arabian J. Chem.* 16 (3), 104563. <https://doi.org/10.1016/j.arabjc.2023.104563>.